Effect of traveling magnetic field on gas porosity during solidification

XU Yan-jin, SU Yan-qing, LUO Liang-shun, LI Xin-zhong,
LIU Jiang-ping, GUO Jing-jie, CHEN Rui-run, FU Heng-zhi

School of Materials Science and Engineering, Harbin Institute of Technology, Harbin 150001, China

Abstract: The effects of traveling magnetic field on degassing of aluminum alloys were investigated, and the critical radius of the pores was calculated. The results show that the critical radius of the pores decreases with increasing the magnetic density linearly when the traveling magnetic field is applied during solidification, and the use of traveling magnetic field promotes the heterogeneous nucleation of pores. After the gas dissolved in the metal liquid accumulates to form large bubbles, the traveling magnetic field forces the bubbles to the surface of molten metal, so the gas is easy to separate from the melt in the liquid stage. The number of pores in the sample decreases with increasing the intensity of traveling magnetic field.

Key words: electromagnetic force; traveling magnetic field; gas porosity; aluminum alloy

1 Introduction

The application of aluminum castings in automotive and aerospace industries has risen significantly in recent years. Therefore, they are seeking methods for producing components with better mechanical properties at reduced cost. One of the most important types of defects that can form in cast products is porosity. There are many types of porosities, but the microporosity is the most severe. Microporosity has a strong negative effect on mechanical properties, especially on ductility and fatigue life, because internal pores act as local stress concentrators and crack initiation sites [1−2]. Thus, the microporosity elimination process is critical to achieving a high-quality final product. Hydrogen is the gas that is appreciably soluble in molten aluminum [3−5]. Several methods are currently used to degas aluminum. These methods include rotary degassing using nitrogen or argon or mixture of either of these with chlorine as a purge gas [5−6], tablet degassing using hexachloroethane [5, 7], vacuum degassing [7−10], and ultrasonic degassing [11−13]. There are two main causes of microporosities in castings: shrinkage porosity due to the volume change in solidification combined with restricted feeding of liquid to the final solidification region; and gas porosity due to the condensation of dissolved gases in the melt frozen, as a result of the difference in solubility of such gases in the liquid and solid phases [1−2]. It is well known that the microporosity is difficult to eliminate because of the hydrostatic tension in liquids. In order to eliminate the microporosity, the pores must be allowed to nucleate and grow up firstly. The role of fluid flow during the solidification of metallic alloys is complex and important, by which both the shrinkage porosity and the gas porosity are affected. Such fluid flow arises from either natural or forced convection. The natural convection is driven by the variations in density, whilst the forced convection can arise from mechanical or electromagnetic stirring [14−15]. However, the mechanisms of the electromagnetic degassing are not yet clear. And fewer work has been done to investigate traveling magnetic field degassing of aluminum alloys. The purpose of this investigation is to assess the effect of the traveling magnetic field (TMF) on the porosity during solidification. With this purpose a traveling magnetic field equipment is developed, the influence of the traveling magnetic field on porosities of hypoeutectic Al-10.3%Si alloy is investigated, and the mechanisms of the traveling magnetic field degassing are discussed.

2 Experimental

The experiment apparatus is based on a traveling

magnetic field generator, which is able to deliver a magnetic flux density of up to 120 mT at the center of a bore with 160 mm in diameter (Fig. 1). It is designed and assembled to hold the sample as firmly as possible when the traveling magnetic fields are induced. The sample, which is cylindrical, with a diameter of 16 mm and a length of 100 mm, was placed in a quartz tube fixed in the center of the bore by a stainless-steel frame with an equipment that controls the cooling rate outside. An electric heating furnace, which was also originally developed for this purpose and was removable through the opening of the upper cylinder, was used to heat and melt the sample. The furnace was removed when the traveling magnetic field generator worked.
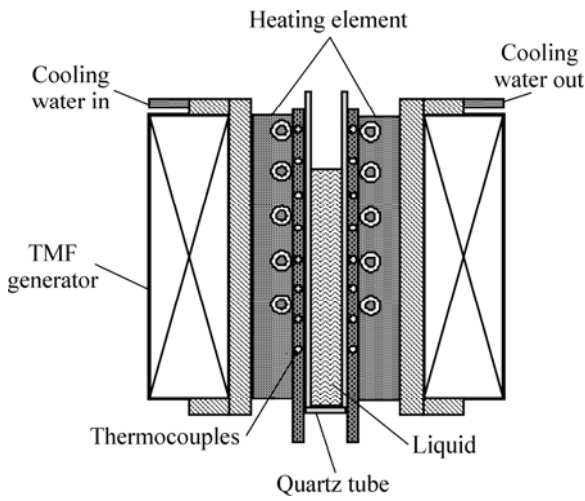

Fig. 1 Schematic of experimental apparatus

The Al alloys were melted in an electric furnace and cast into a graphite mold to produce 16-mm-diameter rods. The rods were then cut into 100 mm long pieces to be used as samples.

Before the magnitude of the traveling magnetic field reached a preset density of 15, 30 and 45 mT, the sample was placed at the center of the traveling magnetic field generator, and the heating furnace was set around the sample and turned on to heat and melt it up to 1 023 K. The molten sample was kept at this temperature for 2 min before the furnace was removed.

3 Result and discussion

3.1 Effect of traveling magnetic field on critical radius of pore

If the local pressure in the liquid is p_e, an amount of work $p_e V$ is needed to push back the liquid away enough to create a bubble of volume V. The formation and stretching of the new liquid/gas interface requires work τS, where τ is the interfacial energy per unit area, and S is the area of the bubble. The work required to fill the bubble with vapor or gas at pressure p_i is negative and

equal to $-p_i V$ [1, 4]. Thus the total work is

$$\Delta G = 4\pi \tau R^2 + (4/3)\pi R^3 (p_e - p_i) \tag{1}$$

where $(p_e - p_i)$ is the pressure difference between the exterior and interior of the bubble, which can be written as Δp for convenience. Similarly to dense phase nucleation, the critical radius R_c in this case is

$$R_c = 2\tau / \Delta P \tag{2}$$

In the case that the TMF was applied, the coil of radius r_c was positioned at z_c, from the formulation calculated by Yesilyurt, the $F_{average}$ is

$$F_{average} = \frac{1}{T}\int_0^T (j_\sigma \times B)dt - \sigma \sum_{i=1}^N \omega_i A_i \times$$

$$\begin{bmatrix} \sum_{i=1}^N \dfrac{\partial(yA_j)}{r\partial r}\dfrac{1}{T}\int_0^T \cos(\omega_i t + \varphi_i)\sin(\omega_j t + \varphi_j)dt \\ 0 \\ \sum_{i=1}^N \dfrac{\partial A_j}{\partial z}\dfrac{1}{T}\int_0^T \cos(\omega_i t + \varphi_i)\sin(\omega_j t + \varphi_j)dt \end{bmatrix} \tag{3}$$

The function $A(r, z)$ is scalar function and given by

$$A(r,t) = A(r,z)\sin(\omega t + \varphi)e_\theta \tag{4}$$

In the case of three coils, and $\omega_1 = \omega_2 = \omega_3 = \omega$, and $\varphi_1 = 0$, $\varphi_2 = 2\pi/3$, $\varphi_3 = 4\pi/3$, Eq. (3) becomes

$$F_{average} = -\frac{\sqrt{3}}{2}\sigma\omega \times$$

$$\begin{bmatrix} A_1\dfrac{\partial(rA_2)}{r\partial r} + A_1\dfrac{\partial(rA_3)}{r\partial r} + A_2\dfrac{\partial(rA_3)}{r\partial r} - \\ A_2\dfrac{\partial(rA_1)}{r\partial r} - A_3\dfrac{\partial(rA_1)}{r\partial r} - A_3\dfrac{\partial(rA_2)}{r\partial r} \\ 0 \\ A_1\dfrac{\partial A_2}{\partial z} + A_1\dfrac{\partial A_3}{\partial z} + A_2\dfrac{\partial A_3}{\partial z} - \\ A_2\dfrac{\partial A_1}{\partial z} - A_3\dfrac{\partial A_2}{\partial z} - A_3\dfrac{\partial A_1}{\partial z} \end{bmatrix} \tag{5}$$

And the pressure p_{TMF} induced by the electric magnetic force is negative, and obtained as:

$$p_{TMF} \approx 2F_{average}\cos\theta / (\pi r^2) \tag{6}$$

For the difference of electrical conductivity between the liquid and the gas, the total work is

$$\Delta G = 4\pi \tau R^2 + (4/3)\pi R^3 (p_e - p_i - p_{TMF}) \tag{7}$$

and the critical radius R_c^* here is

$$R_c^* = 2\tau / (\Delta p - p_{TMF}) \tag{8}$$

When the electromagnetic magnetic field intensities

are 15, 20, 25, 30, 35, 40 and 45 mT, from Eqs. (2) and (8), the R_c^*/R_c values are obtained as shown in Fig. 2. From Fig. 2, we know that the critical radius R_c in the case with TMF is lower than that in the case without TMF. The R_c^* decreases with increasing the magnetic field density linearly. So in the latter case the pores are easy to create and grow up. In fact, the pressures required for nucleation are extremely high. It is clear that the strengths of liquid metals are almost as high as those of solid metals, since their atom structures are similar, and it is difficult to force them apart to create a void for nucleation. When the TMF is applied, the presence of the electric force reduces the surface tension of the liquid metals. For the difference of conductivity between the nonmetal and the metals in the liquid, the liquid metal is pushed away from the nonmetal by the electromagnetic force, and a void is easy to create. So the surface of the nonmetal is not wetted, which is a favored site for the nucleation of the pore. From the classical heterogeneous nucleation theory, we know that not all the inclusions are good nucleation sites for porosities. Those well wetted
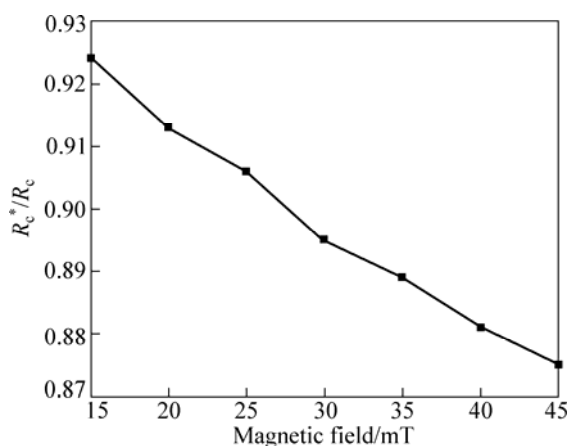
will not be favored. The good nuclei must not be wetted. And when the contact angle exceeds 60° or 70°, the nucleation on the solid surface becomes favorable [1]. So, when the traveling magnetic field is applied during solidification, the critical radius decreases with increasing the magnetic density. And the use of traveling magnetic field promotes the heterogeneous nucleation of pores.

3.2 Effect of traveling magnetic field on distribution of pores during solidification

GERNEZ demonstrated that crystalline solids which had been grown in the liquid, and had never been allowed to come into contact with air, were incapable of inducing effervescence in a liquid supersaturated with gas. Otherwise, the gas dissolved in the liquid metal that will be degassed must be allowed to form a bubble firstly [1]. The role of fluid flow during the solidification of metallic alloys is complex and important for the distribution of the pores. Such fluid flow arises from either natural or forced convection. The natural convection is driven by the variations in density, whilst the forced convection can arise from the traveling magnetic field. In order to access the direct effect of the traveling magnetic field on the distribution of the gas pores, a novel method was designed and carried out. The rods of Al-10.3%Si alloy were prepared. The rods were set into the tube of quartz and was not allowed to come into contact with air. In our experiment, the quartz reacts with the alloy when the liquid metal solidified, and a film appears outside and wraps the rod, so that the gas cannot be degassed out of the tube. Figure 3 shows the surface pores observed by stereoscopy in Al-10.3%Si alloy with an applied traveling magnetic field under different solidification stages. The results show that the application of traveling magnetic field can separate the
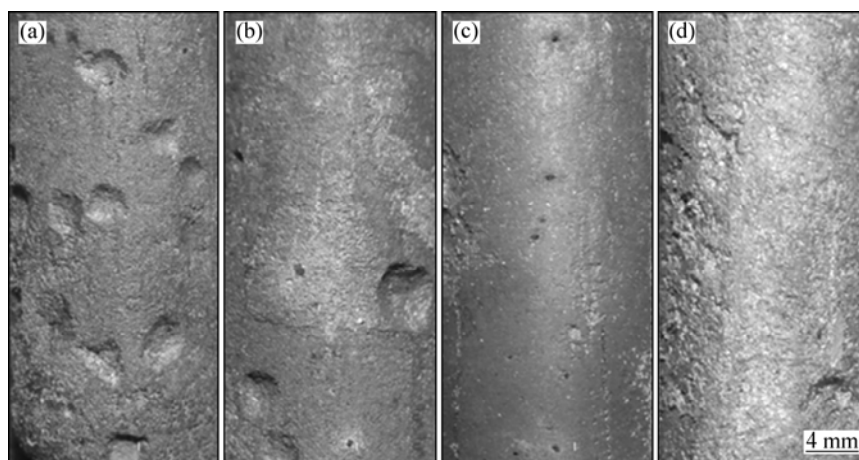
Fig. 2 Curve of R_c^*/R_c with various magnetic field intensity

Fig. 3 Surface pores observed by stereoscopy in Al-10.3%Si alloy with traveling magnetic field under different solidification stages: (a) Applying traveling magnetic field until molten metal is cooled down to 873 K; (b) Applying traveling magnetic field at the early stage (1/3) of solidification; (c) Applying traveling magnetic field at the middle stage (1/3) of solidification; (d) Applying traveling magnetic field at the last stage (1/3) of solidification
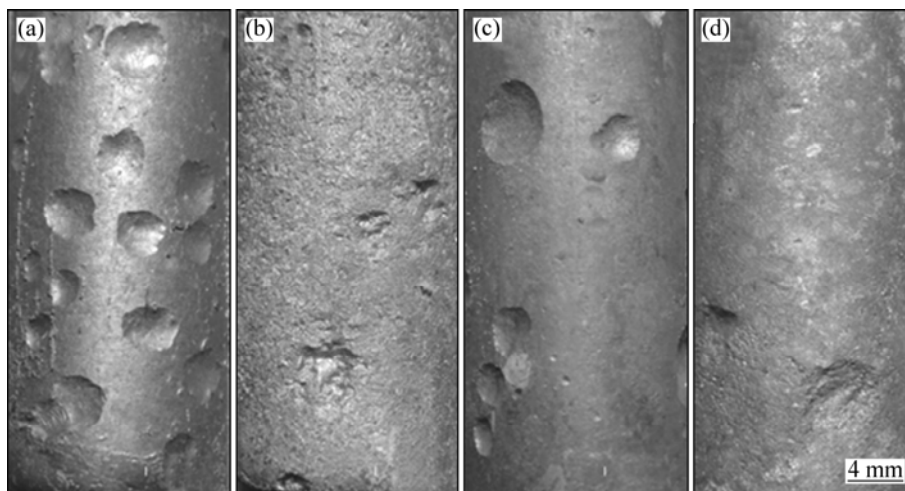
Fig. 4 Surface pores observed by stereoscopy in Al-10.3%Si alloy with traveling magnetic field under different solidification stages: (a) Applying traveling magnetic field until molten metal is cooled down to 873 K and then water-quenching; (b) Without traveling magnetic field until molten metal is cooled down to 873 K and then water-quenching; (c) Applying traveling magnetic field during the crystal growth stage and then water-quenching; (d) Without traveling magnetic field after crystal growth stage and then water-quenching

gas pores from the parent melt to the melt surface effectively. The maximum number of the surface pores can be seen in Fig. 3(a), indicating that in liquid phase stage the gas is easy to separate from the metal liquid. The results shown in Fig. 4 also support the idea above. During the solidification, some gas enriched between the melt and the quartz tube will degas through the gap between the tube and metal liquid. In order to keep the surface pores as many as possible, the sample was water-quenched after the traveling magnetic field treatment. The results show that the traveling magnetic field can separate the gas from the melt, and in the liquid stage, the gas is easy to enrich in the gap between the quartz tube and the metal liquid.

The principle of the traveling magnetic field separation method is that when the melt is exposed to the traveling magnetic field, the electromagnetic force will be induced in the liquid metal but fewer in the gas porosities due to the lower electric conductivity. The schematic diagram of the electromagnetic forces is shown in Fig. 5. The electromagnetic force induced in Al-10.3%Si melt can be described as axial and radial components. When the melt containing gas porosities is exposed to the traveling magnetic field, the electromagnetic Archimedes force will act on the gas porosities because of the difference in the electrical conductivity between the gas porosities and the parent melt, and the direction of the electromagnetic Archimedes force is opposite to the electromagnetic force of the melt. Figure 6 shows the porosity levels in the traveling magnetic field treated samples, which were solidified from 1 023 K at a cooling rate of 30 K/min under the traveling magnetic field intensity of 0, 15, 30,
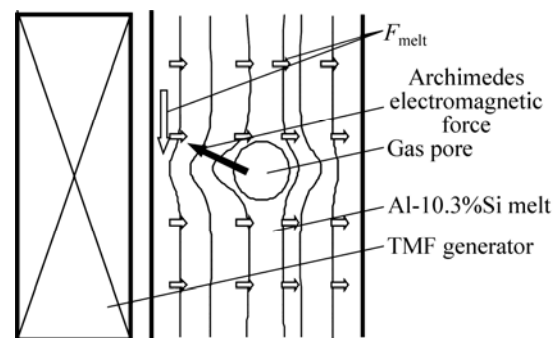

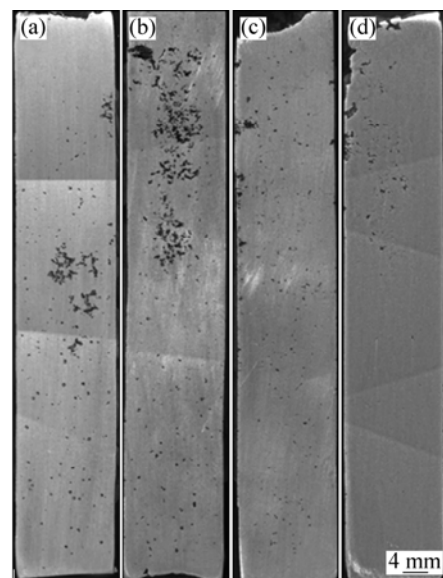**Fig. 5** Principle of traveling magnetic field separation method

Fig. 6 Porosities in Al-10.3%Si alloy with traveling magnetic field under different intensities: (a) 0 mT; (b) 15 mT; (c) 30 mT; (d) 45 mT

45 mT, respectively. The result shows that traveling magnetic field treatment can degas effectively, and the number of the pores in the sample decreases with increasing the traveling magnetic field intensity.

Generally, traveling magnetic field degassing can be divided into three stages: nucleation of cavitation bubbles and growth of the bubbles due to the diffusion of hydrogen atoms from the surrounding melt to the bubbles, coalescence of bubbles to form large bubbles, and the large bubbles moving to the surface of the molten metal and escape of the bubbles at the melt surface.

4 Conclusions

1) When the traveling magnetic field is applied during solidification, the critical radius of pores decreases with increasing the magnetic density. And the use of traveling magnetic field promotes the heterogeneous nucleation of pores.

2) After the gas dissolved in the metal liquid accumulates to form large bubbles, the traveling magnetic field forces the bubbles to the surface of molten metal, so the gas is easy to separate from the melt in the liquid stage. The number of the porosities in the sample decreases with increasing the traveling magnetic field intensity.

References

[1]   CAMPBELL J. Castings [M]. Oxford: Butterworth-Heinemann Press, 2003: 280−396.

[2]   DANTZIG J A, RAPPAZ M. Solidification [M]. Switzerland: EPFL Press, 2009: 479−500.

[3]   CANTOR B, O'REILLY K. Solidification and casting [M]. London: Institute of Physics Press, 2003: 124−235.

[4]   FISHER J C. The fracture of liquids [J]. J App Phys, 1948, 19: 1062−1067.

[5]   SAMUEL A M, SAMUEL F M. Hydrogen evolution during directional solidification and its effect on porosity formation in aluminum alloys [J]. J Mater Sci, 1992, 27: 6533−6563.

[6]   NI Hong-jun, SUN Bao-de, JIANG Hai-yan, DING Wen-jiang. Effects of rotating impeller degassing on microstructure and mechanical properties of the A356 scraps [J]. Materials Science and Engineering A, 2003, 352: 294−299.

[7]   KUZNETSOV V A, KATS Y L. Economical vacuum degassing of steel with the use of mechanical pumps [J]. Metallurgist, 2007, 51: 220−225.

[8]   IWAMOTO K, YAMASAKI M, KAWAMURA Y. Vacuum degassing behavior of rapidly solidified Al-Mn-Zr alloy powders [J]. Materials Science and Engineering A, 2007, 449−451: 1013−1017.

[9]   YAMASAKI M, IWAMOTO K, TAMAGAWA H, KAWAMURA Y, LEE J K, KIM H J, BAO J C. Vacuum degassing behavior of Zr-, Ni- and Cu-based metallic glass powders [J]. Materials Science and Engineering A, 2007, 449−451: 907−910.

[10]   ZHU Xin-wen, JIANG Dong-liang, TAN Shou-hong. Improvement in the strength of reticulated porous ceramics by vacuum degassing [J]. Materials Letters, 2001, 51: 363−367.

[11]   XU H B, MEEK T T, HAN Q Y. Effects of ultrasonic field and vacuum on degassing of molten aluminum alloy [J]. Materials Letters, 2007, 61: 1246−1250.

[12]   XU H B, HAN Q Y, MEEK T T. Effects of ultrasonic vibration on degassing of aluminum alloys [J]. Materials Science and Engineering A, 2008, 473: 96−104.

[13]   XU H B, JIAN X G, MEEK T T, HAN Q Y. Degassing of molten aluminum A356 alloy using ultrasonic vibration [J]. Materials Letters, 2004, 58: 3669−3673.

[14]   GRIFFITHS W D, McCARTNEY D G. The effect of electromagnetic stirring during solidification on the structure of Al-Si alloys [J]. Material Science and Engineering A, 1996, 216: 47−60.

[15]   YESILYURT S, MOTAKEF S, GRUGEL R, MAZURUK K. The effect of the traveling magnetic field (TMF) on the buoyancy-induced convection in the vertical Bridgman growth of semiconductors [J]. J Crystal Growth, 2004, 263(1−4): 80−89.

行波磁场作用对凝固过程中气泡的影响

徐严谨，苏彦庆，骆良顺，李新中，刘江平，郭景杰，陈瑞润，傅恒志

哈尔滨工业大学 材料科学与工程学院，哈尔滨 150001

摘　要：研究行波磁场对铝合金除气行为的影响，计算行波磁场对气泡形核临界半径的影响。结果表明：在行波磁场作用下，气泡的临界形核半径随着电磁场强度的增大呈线性递减，电磁力促进了气泡的非均匀形核，电磁力使得气泡在熔体中长大，并在电磁力的驱动下向熔体的外部溢出。试样中的气泡数随行波磁场感应强度的增大而减少。

关键词：电磁力；行波磁场；气泡；铝合金

(Edited by YUAN Sai-qian)